Chapter 3

Copper-Indium-Gallium-diSelenide (CIGS) Nanocrystalline Bulk Semiconductor as the Absorber Layer and Its Current Technological Trend and Optimization

Nima Khoshsirat and Nurul Amziah Md Yunus

Additional information is available at the end of the chapter

http://dx.doi.org/10.5772/64166

Abstract

The Copper Indium Gallium diSelenide (CIGS) thin film solar cells are considered in this chapter. The interest in $Cu(In_{1-x}, Ga_x)Se_2$ thin film solar cells has increased significantly due to its promising characteristics for high performance and low cost. It is aimed to present an extensive evaluation on CIGS nanocrystalline bulk semiconductor and its application as an absorber layer for thin film solar cells. It is also aimed to improve the CIGS thin film solar cell efficiency through finding optimum ranges of material properties. The first section of this chapter gives an extensive overview on CIGS nanocrystalline bulk semiconductor background and technological trend. In the middle section, a brief review on CIGS Solar Cell processing and challenges are highlighted and the last section a numerical simulation results on the effects of each of constructive nano layer properties on cell performance are shown and compared with valid experimental results.

Keywords: copper-indium-gallium-diselenide (CIGS), indium sulfide (In_2S_3), nanocrystalline, thin film, solar cell, SCAPS

1. Introduction

Thin film solar cells are introduced and developed as the second generation of solar cells to provide high production capacity at lower energy and material consumption [1]. Main motivations for the growth of thin film photovoltaic (PV) are their potential for high-speed and high-throughput manufacturing and minimum material requirements that lead to cost reduction

[2]. This type of solar cell is made on cheap, large area and nonsilicon substrates such as glass, metal foil or plastic.

In 1976, three separate research groups, Panasonic Matsushita, University of Maine and RCA research group had formed the thin-film cell. Each group had used different absorber materials. Consequently, thin film solar cells were divided into three main subcategories based on their absorber materials such as amorphous silicon (a-Si), cadmium telluride (CdTe) and copper-indium-gallium-diselenide (CIGS). All these materials are direct-gap semiconductors that can absorb incoming solar radiation at a thickness much thinner than the required thickness for the silicon wafers in crystalline silicon (Si) solar cells. It is worth noting that the absorption of a-Si, CdTe and CIS/CIGS materials are significantly different. The highest value of solar radiation absorption belongs to CIS/CIGS that can absorb almost complete incoming radiation at first 3–4 μm of the material thickness and 95% of the radiation in its first 0.4–0.5 μm [3].

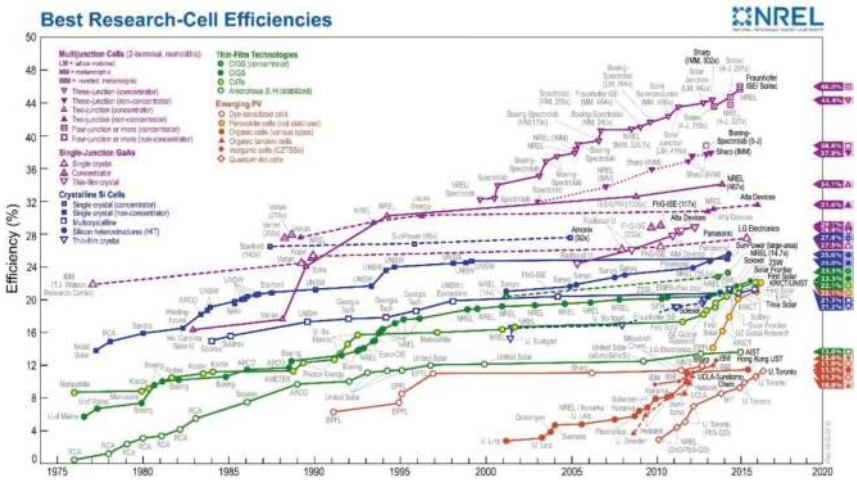

Figure 1. Best research solar cell efficiency released on April 2016 (Lawrence L. Kazmerski, National Renewable Energy Laboratory (NREL) [4].

Figure 1, which was recently published by US National Renewable Energy Laboratory (NREL), shows the best researched solar cell efficiencies that have been reported so far [4]. It can be observed that there is an efficiency gap between mono (single)-crystalline Si and poly-(multi)crystalline Si cells. Both of these silicon-based solar cells show higher levels of efficiency in comparison with other generations of solar cell. As a third-generation solar cell, the dye-sensitized cells have reached to over 10% efficiency for laboratory sample, but in general, their efficiency is less than other types of solar cells and are still known as an emerging PV technology. Among thin film solar cells, the CIGS cell has the highest record by the efficiency of over 20% (22.3% for a cell with glass substrate [4] and 20.4% for a cell with polyimide foil substrates [5]). The highest CdTe efficiency record is 22.1% [6], which is 0.2% lower than CIGS

http://dx.doi.org/10.5772/64166

on glass substrate. Nevertheless, it needs to be studied and developed more in order to be successfully transferred from the laboratory stage to commercial stage and stay competitive in the PV market.

2. CIGS cell structure

Copper-indium-gallium-diselenide (CIGS) thin-film solar cells are multilayer thin film devices with $Cu(In_{1-x}\ Ga_x)Se_2$ nanocrystalline bulk semiconductor as the absorber material. The cheap substrate and monolithic interconnection of individual cells in a module are some initial advantages of CIGS thin film solar cells in comparison with silicon wafer-based solar cell. The suitable energy band gap of CIGS is another benefit of this compound semiconductor. Theoretically to ensure a sufficient absorption of the solar irradiation, the band gap of the absorber should be within the range of 1.0–1.8 eV with the optimum value of 1.5 eV [7]. The energy band gap of $Cu(In_{1-x}\ Ga_x)Se_2$ can be varied from 1.06 to 1.7 eV depending on the Ga/(Ga+In) ratio. Thus, the CIGS quaternary compound semiconductor is a good option to be used as an absorber material in solar cells.

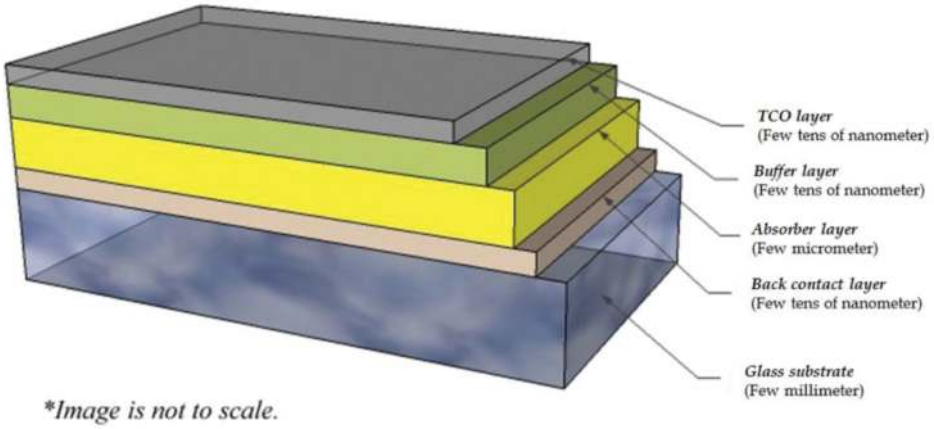

Figure 2. Typical CIGS thin-film solar cell structure [9].

Figure 2 shows the structure of CIGS solar cell. In this structure, the device is formed on low price substrates such as glass, polyimide foils, stainless steel, etc. The most common material used for substrate in CIGS technology is soda lime glass (SLG) due to its smooth surface, stability, electrical insulating features and more importantly its affordable price [8].

2.1. Back contact

The metal back contact is the first layer to be deposited on the substrate. This layer plays the role of an optical reflector as well as a contact for delivering the carriers to the load. Several

materials have been proposed for the back contact such as molybdenum (Mo), tungsten (W), tantalum (Ta), manganese (Mn), titanium (Ti), etc. The most common material used for the back contact is molybdenum (Mo) (especially for soda lime glass substrates). This is because of molybdenum has low contact resistance to the absorber layer and it is stable at the processing temperature. These can limit the diffusion of atoms and hence minimize the destructive reactions during CIGS growth [10]. The process condition and growth parameters in the electrical and structural properties of Mo contact are important in the deposition method. For instance, although the resulting electrical resistivity of the Mo layer deposited at the low-pressure process is low, its adhesion to the substrate is poor and can be easily peeled off from the substrate's surface [11]. Thus, a compromise between the layer's adhesion and its resistivity is required during the back contact deposition.

2.2. Absorber layer

The absorber layer is deposited on the top of back contact layer as shown in **Figure 2**. $Cu(In_{1-x}Ga_x)Se_2$ is one of the most promising absorber material for PV applications. It is a direct band gap semiconductor. Its energy band gap (E_g) is within the range of 1.06–1.7 eV. The exact value of E_g depends on Ga/(Ga+In) ratio. The Cu concentration in the composition can also cause changes to CIGS band-gap value. A decrease in Cu concentration can cause an increase in band gap [12]. CIGS application in solar cells started with growth and the structural characterization of $CuInS_2$ (CIS) with the energy band gap of 1–1.06 eV in 1953. Then, some researches were conducted to increase the CIS band gap to the theoretical optimum value of around 1.4–1.5 eV. It was found that by adding gallium (Ga) to CIS will keep the overall number of group-III atoms, while In + Ga constant could lead to an increase in band gap [13]. This finding opens a new path for the enhancement of CIGS solar cell through adjusting the absorber layer band gap.

2.3. Buffer layer

The next layer in the CIGS solar cell structure is the buffer layer. This layer is deposited on the top of the absorber layer. The role of a buffer layer in the heterojunction is to form a junction with the absorber layer while leading maximum amount of incoming light to the absorber layer. The buffer layer should have a minimal absorption loss, low surface recombination and electrical resistance in photogenerated carriers driving out [14]. The most important features of the buffer layer are to protect the junction against chemical reactions and mechanical damage. It is also to optimize the band alignment of the cell, electrical properties and making a wide depletion region with p-type absorber layer. This will eventually minimize the carriers tunneling and maintain higher open circuit voltage value and later establish a higher contact potential [15]. In order to satisfy such desired features, the buffer layer should have a wider band gap in comparison with CIGS layer. In addition, the deposition process for the buffer layer should passivate the surface states of the absorber layer and provide a suitable conduction band alignment with the absorber to achieve higher efficiency [16]. The first experimental thin-film solar cell device using CIS absorber layer was an heterojunction between a p-type CuInSe layer and a thin layer of n-type CdS compound semiconductor. Further development

http://dx.doi.org/10.5772/64166

of this structure was the vacuum evaporation of an undoped CdS layer, followed by indium-doped CdS layer to increase cell's performance and efficiency. Furthermore, the doped CdS would play the role of a transparent conductor layer [17]. The most efficient CIGS solar cell fabricated so far used CdS buffer layer. Although CdS buffer layer has yielded high-efficiency cell, its toxicity [18], incompatibility with in-line vacuum-based production method [19] and low-performance level of CdS/CIGS cells in short wavelength domain [20] led researchers to think about replacing CdS with a nontoxic material. At present, the development of Cd-free wide-band gap buffer layer is one of the main objectives in the field of CIGS thin film solar cells. The development of Cd-free device was initiated in 1992, and many different materials were proposed for it until now. These materials generally can be categorized in two main groups of zinc (Zn) based such as ZnS, ZnSe, ZnO, (Zn,Mg)O and indium (In) based including $In(OH)_3$, In_2S_3, In_2Se_3 [21].

2.4. Window layer

A thin layer of transparent conductive oxide (TCO) as front contact is just next to a buffer layer. This TCO layer should have a sufficient transparency to let most part of incoming light through the underlying layers. It must also have sufficient conductivity in order to transport the photogenerated current to the external circuit with minimum resistivity loss [22]. The most common used TCO material in CIGS solar cells is highly doped zinc oxide (ZnO) with the energy band gap of above 3.3 eV [23]. A doping of the ZnO layer is usually obtained by group III elements, exclusively with aluminum [24].

3. Criteria of material selection for the CIGS thin-film solar cell

There are some parameters that should be taken into consideration while choosing the material for different layers of a CIGS thin-film solar cell. The parameters such as the band gap, electron affinity, absorption coefficient, carrier concentration and many more can affect solar cell's characteristics and its output performance. The most effective parameters are the band gap and the electron affinity that will be discussed in the following sections.

3.1. Band gap

The most important parameter in CIGS solar cell is the absorber layer band gap. According to the theoretical considerations proposed by Loferski [25], the band gap values within the range of 1.4–1.5 eV is ideal for the absorber layer. **Figure 3** shows the maximum theoretical conversion efficiency as the function of semiconductor band gap for different absorber materials. Furthermore, the absorber layer should be a p-type and direct band gap semiconductor to have maximum conversion efficiency. This p-type semiconductor is proposed due to its longer electron diffusion length [26].

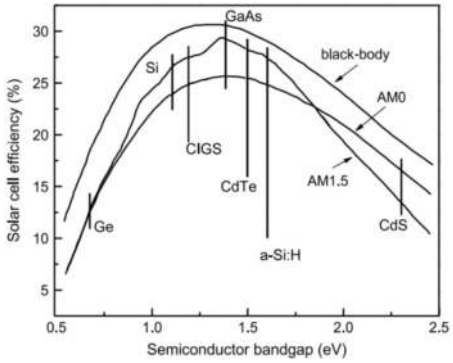

Figure 3. Theoretical maximum achievable efficiency versus absorber material band gap [25].

The energy band gap is also an important criterion for choosing a proper material for buffer and window layers. In this case, the energy band gap (E_g) needs to be adequately larger than absorber band gap to absorb as less photons as possible. It is assumed that photons with energies equal to and greater than the semiconductor material band gap can be absorbed in that material. In a CIGS solar cell, the light first passes through the window layer and those photons with energies more than the window layer's band gap will be absorbed in this layer. The remaining photons then pass through the buffer layer, and similarly, a part of incoming photons that have energies higher than the buffer band gap will be absorbed in the buffer layer. Most of the photogenerated carriers in the window and buffer layer cannot be collected due to their low mobility. **Figure 4** shows the photon flux at standard AM1.5 solar spectrum as a function of wavelength and maximum possible short circuit current density (Jsc) that can be generated in a solar cell as function of absorber material band gap. As it can be seen, the

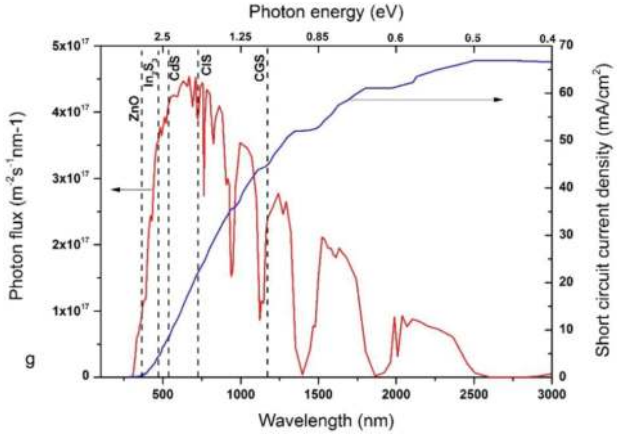

Figure 4. Photon flux at standard AM1.5 solar spectrum; maximum possible short circuit current density (Jsc).

http://dx.doi.org/10.5772/64166

photogenerated current loss is less than 1 mA/cm due to the absorption of photons in ZnO transparent conductive oxide (TCO) layer. Therefore, the loss of current caused by the absorption of light in the buffer layer is about 4 and 8 mA/cm^2 for In_2S_3 and CdS buffer materials, respectively.

In a cell with CIS absorber material in which its band gap is 1.06 eV as shown in **Figure 4**, the maximum photogenerated short-circuit current density (Jsc) is about 46 mA/cm^2, which is around 22 mA/cm^2 higher than maximum short-circuit current density in a cell with CGS absorber layer. Thus, although the band gap is not the only parameter, which can affect the cell performance, the selection of material for different layers in a solar cell should be under the band gap theoretical considerations in order to have the maximum absorption of light in absorber layer and minimum current loss.

3.2. Electron affinity

Another important parameter is electron affinity (X_e). The difference between electron affinity of absorber and buffer layer has an important role in the band alignment and shaping the discontinuity of energy band at the buffer/absorber interface. The discontinuity of conduction band at the interface that is called conduction band offset (CBO) can be positive (spike) or negative (cliff). This is due to the difference between absorber and buffer electron affinity. **Figure 5** shows the band alignment and formation of cliff and spike conduction band offset in CIGS solar cell. A cliff CBO at absorber/buffer interface can cause a reduction in open-circuit voltage (Voc) because of the lack of barrier height [27]. A positive CBO (spike) inhibits the flow of photogenerated carriers from the absorber to the buffer. A large spike makes a large barrier for carriers and therefore reduces the Jsc. However, a small spike does not act as a barrier [28]. Thus, the electron affinity of absorber and buffer layer should be compatible based on their energy band gap to maintain suitable levels of open-circuit voltage and short-circuit current density.

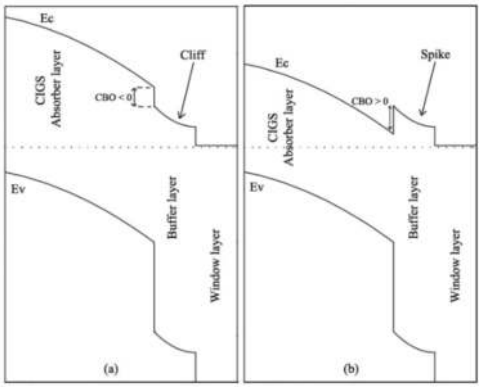

Figure 5. Band alignment between absorber and buffer layer. Conduction band offset: (a) Cliff and (b) Spike [20].

3.3. Quantum efficiency (QE)

Quantum efficiency is used as a tool for measuring the spectral response of the device. It gives a detail information about the absorption of photons and creation of carriers at different wavelength or photon energy levels. It is defined by the ratio of electrons collected from the device per incident photons at each wavelength:

$$QE\ (\lambda) = \frac{Number\ of\ collected\ electrons}{Number\ of\ incident\ photons} = \frac{I(\lambda)/q}{\varphi_p(\lambda)}$$

where the $I(\lambda)$ and $\varphi_p(\lambda)$ are photogenerated current and photon flow, respectively. Quantum efficiency is a relative value and its optimum number is 1 (i.e., 100%) for all wavelengths below the corresponding wavelength to the absorber band gap and zero for wavelength above it, but in reality, it is always less than 100%. **Figure 6** shows a typical CIGS cell's quantum efficiency (QE) curve and the loss mechanisms that can cause decreases in quantum efficiency. As shown, the reflection is one mechanism that decreases the quantum efficiency of the cell. It can be caused by light reflection at material interfaces or partial coverage cells' front surface that is made by front electrode.

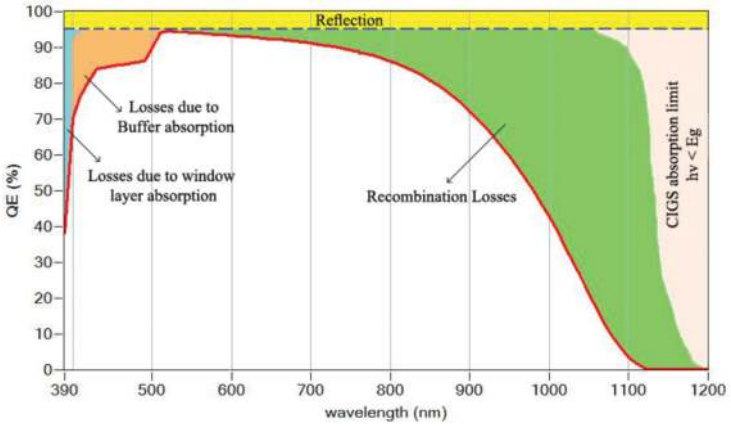

Figure 6. A typical cell's quantum efficiency curve and loss mechanism.

The other loss mechanism, which has destructive effect on cells' quantum efficiency, is the absorption of photons in the short-wavelength (UV) region. This arises from the absorption of light in buffer and window layer. The absorption in transparent conductive oxide window layer is typically low. This is due to the high-energy band gap of the materials that are usually used for this layer. But the buffer layer absorption is one of the major losses source in CIGS solar cells. As can be seen, there is a limitation at long wavelength because of the limit of the absorber layer absorption, which is based on its energy band gap. The short-circuit current

http://dx.doi.org/10.5772/64166

and consequently the short-circuit current density of the cell can be obtained from the quantum efficiency:

$$J_{sc} = \int_{\infty}^{\lambda} G_{\lambda}(\lambda).QE(\lambda)d\lambda$$

where G_{λ} is the spectral irradiance of the reference distribution.

3.4. Recombination rate

The generation of carriers is counteracted by the carriers' recombination. The recombination phenomenon is the process, which acts to bring the solar cell back to equilibrium by the combination of exited electrons and holes. During the recombination, an electron relaxes back to the valence band from the conduction band by giving its energy to a photon or a phonon. While the electron transfers its energy to a photon in a single step, its energy will be divided and transferred to several phonons in several steps. There are three main mechanisms of recombination in a solar cell that can relax back the electrons from the conduction band to the valence band including radiative recombination, auger recombination and Shockley-Read-Hall (SRH) recombination [29]. The radiative mechanism happens when an electron gives its energy to a photon and emits it with this excess energy. Auger recombination mechanism includes the recombination of electron and hole and transferring the excess energy from the electron to the third carrier. The third recombination mechanism is Shockley-Read-Hall (SRH) recombination that includes emission of one or several phonons by transferring the excess energy of electron to them. In this mechanism, since the phonons' energy is ≤0.1 eV, band-to-band recombination requires simultaneous multiple phonon involvement. The SRH recombination usually involves defects states in the volume and at surfaces of the material. It is significant that the SRH recombination is the dominant recombination mechanism for CIGS solar cells due to the existence of defects in CIGS material. The recombination rate, R, is given by the classical Shockley-Read-Hall (SRH) description:

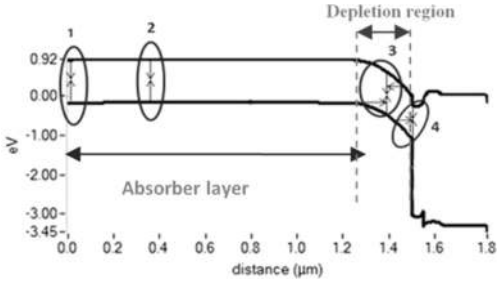

Figure 7. Band diagram and recombination paths in a CIGS solar cell: (1) Recombination at back contact. (2) Recombination at quasi neutral region. (3) Recombination in the space charge region (SCR). (4) Recombination at the interface.

$$R_{srh} = \frac{np - n_i^2}{\tau_{n_0}(n + n_1) + \tau_{p_0}(p + p_1)}$$

where the τ_{n_0} and τ_{p_0}, respectively, are the electron and hole minimum lifetime in the case of completely unoccupied defect states. The n_1 and p_1 are the electron and hole density, respectively, when the Fermi level lay at the energetic position of the defect. Furthermore, the recombination in thin film chalcopyrite solar cells (e.g., CIGS solar cells) can be categorized based on the place where it happens. There are four main recombination regions, including the recombination at the back contact (BC), quasi-neutral bulk, space charge region (SCR) and recombination at the interfaces (IFR). **Figure 7** represents the recombination regions in the band diagram of a CIGS solar cell. Region 1 represents the recombination at back contact and region 2 shows the quasi-neutral recombination (QNR) in the absorber layer. Region 3 is the place, where the recombination at space charge region (SCR) occurs, while region 4 is the place of recombination at the absorber/buffer interface happens. At each operation condition and cell structure, one of these recombination mechanisms is dominant. The basis of determination of the dominant recombination path in a CIGS solar cell is that, for all recombination paths, the diode saturation current density (J) can be written as below.

$$J_0 = J_{00} e^{\left(\frac{-E_a}{AKT}\right)}$$

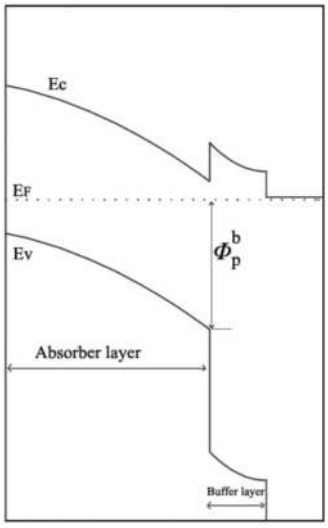

Figure 8. Interface barrier for holes at the absorber/buffer interface that is the energy distance between Fermi level and valence band edge at the absorber/buffer interface.

http://dx.doi.org/10.5772/64166

The J_{00} is the temperature-independent prefactor, E_a is the activation energy, "A" is the diode ideality factor that is the function of temperature and KT is the thermal energy. The most important parameter among these parameters is the activation energy that is dependent on the path of recombination. For the recombination in quasi-neutral balk (QNR) and recombination in space charge region (SCR), the activation energy (E_a) is equal to the energy band gap (E_g). In case of recombination at the absorber/buffer interface (IFR), E_a is equal to interface barrier for holes (φ_p^b). The interface barrier for holes normally is lower than the band gap. The (φ_p^b) that is shown in **Figure 8** is actually the energy distance between Fermi level (E_F) and valence band edge at the absorber/buffer interface.

4. A brief review on CIGS solar cell processing

CIGS thin-film solar cell fabrication process starts from the deposition of back contact layer onto the substrate. The condition of the process and growth parameters plays an important role in the electrical and structural properties of back contact layer. Therefore, the processing setup should maintain the desired resultant layers' features such as low resistivity and high adhesion to the substrate. The compatible deposition methods that are used to deposit molybdenum (Mo) as the common used back contact material are evaporation and sputtering [30, 31].

The second layer that should be deposited is the CIGS absorber layer. The essential criteria to select the processing technique of absorber layer are growth controllability, high deposition rate, reproducibility and low cost. Thus, several deposition techniques and growth methods are used for the absorber layer since the beginning of CIGS thin-film technology. There are advantages and disadvantages for each technique particularly for the criteria that are mentioned earlier. The CIGS deposition techniques can be divided into two main categories of high-cost vacuum-based technique and low-cost nonvacuum-based processing technique [32]. The vacuum-based deposition techniques, which are commonly used in CIGS deposition, are as follows [33]:

- Thermal evaporation such as coevaporation from pure elemental metals.
- Sputtering from metal selenide targets.
- Selenization of metal precursors.
- A hybrid of the above processes.

Although the vacuum deposition technique is applied to fabricate the commercialized CIGS cells and also the best laboratory-scale CIGS cell, there are some other low-cost CIGS thin film deposition techniques that are nonvacuum processes. Some of these techniques, which lead to fabricating a cell with an acceptable efficiency level, are the hydrazine-based deposition [34], screen printing [35], spray deposition [36], dip-coating [37], pulsed laser-assisted deposition (PLAD) [38], electrodeposition [39], etc. The considerable challenges in each alternative deposition and formation methods are producing CIGS layer, free from destructive concen-

trations of impurities and controlling the Ga concentration profile across the CIGS absorber. Both are effective factors on device efficiency [40].

The most commonly used deposition technique for the buffer layer in CIGS thin-film solar is the chemical-bath deposition (CBD) that is a low-cost, large-area process [41–43]. Since the chemical bath deposition technique is incompatible with in-line vacuum-based production method, which is used for commercialized CIGS solar cell fabrication in industry, several alternative deposition techniques were proposed for buffer layer deposition process. These alternative methods are sputtering, atomic layer deposition (ALD), metal organic chemical vapor deposition (MOCVD), an ion layer gas reaction (ILGAR), a molecular beam epitaxy (MBE), etc. Each method may have some advantages and disadvantages, so a compromise between desired features and possible drawback is required. For instance, the atomic layer deposition (ALD) is a chemical vapor deposition method with very good thickness controllability and film uniformity; however, its weakness is the low growth rate in comparison with the other techniques [44]; while, the MOCVD is known as a fast and reliable deposition method. It can be integrated into in-line processes, but the MOCVD involve low controllability of impurity concentration across the layer. It is used for the deposition of zinc (Zn)-based buffer layers' deposition and the 13.4% efficiency was obtained from a $Cu(In,Ga)(S,Se)_2$ solar cell with a 20-nm MOCVD deposited ZnSe buffer layer [45].

Various deposition methods have been tested for TCO films such as RF or DC magnetron sputtering [46, 47], the sol-gel method [48], chemical vapor deposition (CVD) [49], pulsed laser deposition [50] and electrodeposition [51]. The TCO layers' deposition technique should be in low-temperature i.e. lower than 150°C. This is to avoid the detrimental interdiffusion across the underlying chalcopyrite layers. It also should be compatible with CIGS cells' in-line processing steps. Hence, magnetron sputtering of ZnO is the most commonly used deposition technique of TCO films among the above-mentioned processing methods. Magnetron sputtering is in a moderate price and consumes low temperature along with well controllable thickness and doping concentration. The RF magnetron sputtering is usually used for small area and laboratory-scale cell. But for the large-scale industrial production, the DC magnetron sputtering is used [52, 53].

5. CIGS thin-film solar cell challenge

Although the CIGS thin-film solar cell has already reached a technical maturity level that made it able to enter a mass production, there is still a large gap between the best commercial CIGS module efficiency of 12% [54] and the highest laboratory-scale efficiency of over 22%. Besides, there are some questions about the optimum cell structure, material properties and many more. These should be answered and explained in order to develop further the CIGS thin-film solar cell. Those unanswered questions arise obviously from an incomplete theoretical understanding about the cells.

In comparison with other types of solar cell, the CIGS cell is much more complex. This complexity comes from the nature of materials that are usually used in this type of solar cell.

http://dx.doi.org/10.5772/64166

Those materials are all compound semiconductors with tunable material properties. The other reason that makes the CIGS solar cells much more complex is the number of layers used in the cell structure. Thus, the complex fundamental semiconductor equations should be applied to all these layers with different material properties. That is why the study of this type of solar cell seems to be difficult and the theoretical understanding about some phenomenon in the CIGS cell's formation and operation are still under study. There are two major challenges that are briefly discussed below.

5.1. Defect nature

CIGS is a p-type semiconductor that is doped by intrinsic defects. In a CIGS bulk, there are vacancies such as V_{Cu}, V_{In}, V_{Se}, etc. and antisite defects like In_{Cu}, Cu_{In}, Ga_{Cu}, Cu_{Ga}. Some of these defects cause p-type doping such as V_{Cu} and some others may add n-type doping such as V_{Se} or $In_{Cu.}$ Theoretical and experimental studies have been done on CIGS intrinsic defects [55–57]. The results show that the copper vacancies dominate in CIGS and the p-type nature of this compound semiconductor arises from this defect. Although it is known that gallium (Ga) content can improve the CIGS electro-optical properties, but high Ga ratio could cause efficiency degradation. The physics behind this phenomenon is still under debate but one of the most possible reasons in antisite defects related to Ga. It is also identified that the diffusion of Na from the glass substrate to the absorber layer increases the carrier concentration in CIGS layer. This leads to a formation useful defect cluster such as the upgrading of CIGS material properties. However, more comprehensive understanding from the origin of defects and their contribution to CIGS electro-optical properties are still required.

5.2. Buffer layers

The highest demonstrated efficiency of CIGS solar cell has been obtained by a cell with a chemical bath-deposited (CBD) cadmium sulfide (CdS) buffer layer. Nevertheless, the cadmium is classified as a toxic material. Thus, a Cd-free buffer layer needs to be investigated and developed. Although, with the appropriate safety rules in fabrication process, the exposure to the cadmium can be avoided, due to breaking or disposal of cadmium containing products, the release of cadmium in the cell has a destructive effect on the environment and human health. Therefore, from July 1, 2006, two directives were regulated on the use of toxicants and heavy metals such as Hg, Cd, Pb in electronic products within the European Union: Directive on the Restriction of the Use of certain Hazardous Substances in Electrical and Electronic Equipment (RoHS) and Waste Electrical and Electronic Equipment Directive (WEEE) [58, 59]. Hence, in order to avoid the toxic heavy metal containing waste in solar cells, examining Cd-free buffer layers is necessary. Nontoxicity will ensure that stringent legislation relating to the use and disposal of toxic material cannot be an obstacle to improve the CIGS thin-film solar technology. In addition to the environmental problems, CdS buffer layer causes poor short-wavelength response due to absorption of the UV lights. This prevents high energy photons to reach the absorber layer and consequently reduces the quantum efficiency of the cell in UV region. Therefore, using an alternative buffer material or elimination of buffer layer

in such a way can enhance the quantum efficiency with environmental friendly materials. These are other challenges of CIGS thin-film solar cells.

Absorber	Window	η (%)	Voc (v)	Jsc (mA/cm^2)	FF (%)	Area (cm^2)	Ref.
CuInS2	i-ZnO/ZnO/Al	13.5	0.604	30.6	73	25	[63]
CuInS2	i-ZnO/ZnO/Al	14.7	0.574	37.4	68.4	0.5	[64]
$Cu(In,Ga)Se_2^*$	i-ZnO/ZnO/Al	13.3	0.606	29.6	74	0.5	[65]
$Cu(In,Ga)Se_2$	i-ZnO/ZnO/Al	11.1	0.652	24.7	69.1	0.5	[66]
$Cu(In,Ga)Se_2$	i-ZnO/ZnO/Al	13.3	0.637	28.8	72.3	0.5	[67]
$Cu(In,Ga)Se_2$	i-ZnO/ZnO/Al	16.4	0.665	31.5	78	0.1	[68]
$Cu(In,Ga)Se_2$	i-ZnO/ZnO/Al	2.88	0.5136	30.83	47.65	3.75	[69]
$Cu(In,Ga)Se_2$	i-ZnO/ZnO/Al	12.1	0.66	26.9	68.4	25	[70]
$Cu(In,Ga)Se_2$	i-ZnO/ZnO/Al	12.3	0.525	31.8	73.6	0.5	[71]
$Cu(In,Ga)Se_2$	i-ZnO/ZnO/Al	14.1	0.648	34.3	63.3	0.5	[72]
$Cu(In,Ga)Se_2^*$	i-ZnO/ZnO/Al	12.4	0.556	31	72	6.25	[73]
$Cu(In,Ga)Se_2$	i-ZnO/ZnO/Al	10.8	0.592	29.5	62	900	[74]
$Cu(In,Ga)Se_2$	i-ZnO/ZnO/Al	12.9	0.662	26.8	72.6	900	[75]
$CuGaSe_2$	ZnO/Al	6	0.625	11.5	83	0.5	[76]
$CuGaSe_2$	ZnO/Al	3.9	0.785	14.5	34.3	0.5	[76]

Table 1. Summary of the Cd-free CIGS solar cell and modules with In_2S_3 buffer layer.

Development of Cd-free buffer layer for CIGS solar cell started in 1992 with an efficiency level of about 9% [60, 61]. Investigations during last decades show that some Cd-free material such as In_2S_3, ZnS and $Zn_{1-x}Mg_xO$ can potentially be used as alternative buffer layers in CIGS solar cells. The major advantage of these materials is that their band gap is larger than CdS band gap. It is worth noting that the In_2S_3 present a wide range of energy band gap from 2.1 to 2.9 eV [62]. In comparison with CdS, cells that use buffer materials with higher band gap have better spectral response in short wavelength due to less blue absorption loss in the buffer layer. **Table 1** shows the summary of Cd-free CIGS solar cells and modules that used In_2S_3 as one of the most promising alternative materials for the buffer layer.

The data shown in **Table 1** indicate that wide ranges of efficiency have been reported for the cells, which used same materials in absorber, buffer and window layer. These differences in efficiency value of the cells arise from differences in processing techniques, cells' geometrical and electro-optical properties of constituent layers. For instance, the cells that are shown with star mark (*) in **Table 1** are made by Cu(In, Ga)Se_2 absorber, In_2S_3 buffer and i-ZnO/ZnO/Al window layer. Both cells are made by same processing techniques but represent different efficiency (12.4 and 13.3%). The differences that are clearly reported for these samples are in

http://dx.doi.org/10.5772/64166

buffer layer thickness and band gap. The cell with the efficiency of 12.4% used a 50-nm buffer layer and the other one used 90-nm buffer layer. In one sample, they tried to control the oxygen content in buffer layer, and in another, they neglected it. These cells may have other differences in terms of absorber or window layer's properties. Thus, in parallel with ongoing efforts for mass production, it is necessary to optimize the cells in terms of layers' geometrical and materials' electro-optical properties in order to develop the CIGS thin film solar cells further. Solar cells' modeling and simulation are those beneficial approaches to reach an optimized cell. In other words, the cell performance can be simulated under different conditions by considering the independent and dependent parameters and the optimized cell can be concluded from superposition of simulation results.

6. Performance of the optimized CIGS solar cell through simulation

In this section, all the obtained optimized ranges that are reported in published results [9, 77–81] are used to evaluate the performance of a CIGS solar cell with optimum layer properties. This evaluation was done for the cells with uniform and graded band structure separately. **Figure 9(a)** shows the output parameters and the J–V characteristics of the cell with uniform band structure and optimized material properties, under dark and illuminated conditions. As shown, the efficiency of 20.16% is achieved through the simulation from this CIGS solar cell, which is higher than the best reported efficiency of a CIGS/In_2S_3/i-ZnO/ZnO/Al solar cell is 16.4% [68]. According to the simulation results and analysis, which are given in previous sections, the cell's open circuit voltage is enhanced by setting the absorber layer band gap at optimum value (1.2 eV). The cell's short-circuit current density is improved by setting the absorber layer thickness at optimum value (2±0.5 μm) and also by decrease in buffer and window layers' thickness that leads to the increase in absorber layer's absorption rate and decrease in buffer and window layers' recombination rate. The fill factor is also upgraded by setting the absorber layer band gap and thickness at optimum value and decrease in buffer

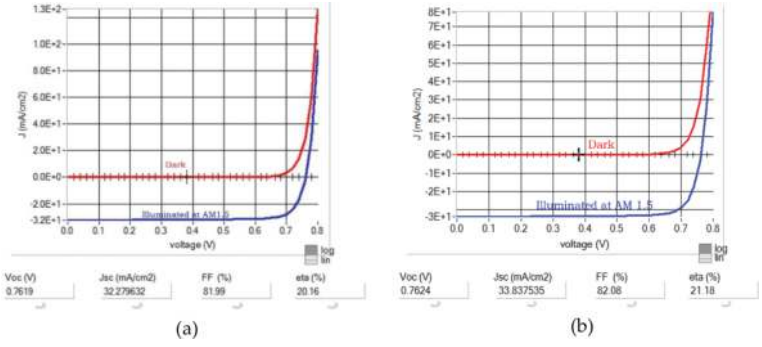

Figure 9. J–V characteristics and the output parameters of the optimized cell under dark and illuminated conditions: (a) cell with uniform band structure, and (b) cell with graded band structure.

and window layers' thickness. A cell with optimum parameters and graded band absorber and buffer layer was also examined. The output characteristics of the cell with graded band structure and optimized material properties are shown in **Figure 9(b)**. As expected, it represents higher performance in comparison with the cell that has uniform band structure.

Cell	Material properties			Cells' output measurements						
	CIGS layer thickness (μm)	CIGS layer band gap (eV)	In_2S_3 layer thickness (μm)	In_2S_3 layer band gap (eV)	ZnO/Al layer thickness (μm)	ZnO/Al layer band gap (eV)	Voc (V)	Jsc (mA/cm²)	FF (%)	Efficiency, η (%)
Best cell reported in literatures [67]	2	N.A	0.03	2.7	0.1	N.A	0.665	31.5	78	16.4
Simulation results for the best cell reported in literatures	2	1.14–1.27	0.03	2.7	0.1	3.42–3.68	0.665	31.5	78	16.4
Simulated cell with uniform band structure	2	1.2	0.04	2.5	0.08	3.86	0.762	32.28	81.99	20.16
Simulated cell with graded band structure	2	1.2–1.7	0.04	2.5	0.08	3.86	0.762	33.84	82.08	21.18

Table 2. Summary of simulated cells' properties in comparison with the best reported cell.

Table 2 shows the summary of material properties that were used in simulated cells plus the best experimental and laboratory-scale CIGS/In_2S_3 cell's property, reported in the literature with their output measurements under the standard AM1.5 solar spectrum and environment temperature of 300°K. The differences in open-circuit voltage and the efficiency may arise from the difference in absorber and TCO layers' band gap, which is not reported for the experimental cell in the reference [68]. A cell with same parameter settings as used and reported in experimental reference was simulated and the results are also shown in **Table 2**.

As the proof of the present study, the best experimental cell with the settings that are mentioned in reference [68] was simulated to find approximate and possible ranges of unknown variables; CIGS layer and ZnO layer energy band gap. The simulation was performed by varying the CIGS and ZnO layers' band gap while the other independent parameters were kept constant. **Figure 10** shows the simulation results in the form of efficiency as the function of absorber and window layers' energy band gap in a color map.

http://dx.doi.org/10.5772/64166

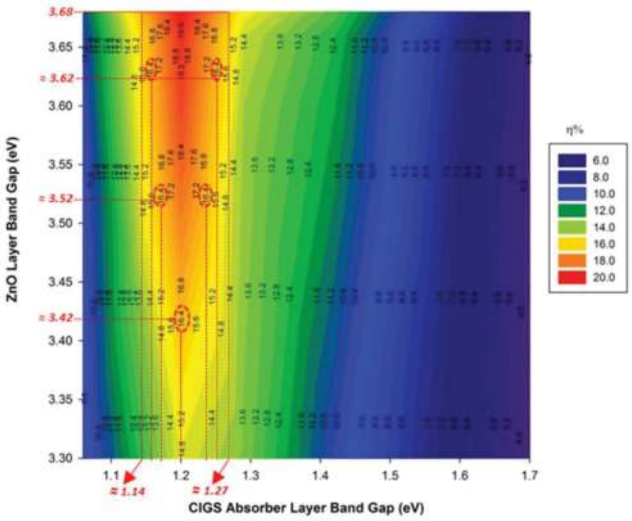

Figure 10. Simulation of best experimental cell: efficiency as the function of absorber and window layers' energy band gap.

Layer parameters	CIGS	In_2S_3	i-ZnO	n-ZnO
Thickness (μm)	2	0.04	0.07	0.08
E_g **(ev)**	1.2	2.5	3.3	3.68
X_e **(ev)**	4.25	4.25	4.6	4.24
ϵ_e	13.6	13.5	9	9
N_c **(1/cm³)**	2.2E+18	1.8E+19	2.2E+18	2.2E+18
N_v **(1/cm³)**	1.8E+19	4.0E+13	1.8E+19	1.8E+19
μ_n **(cm²/Vs)**	100	400	100	100
μ_p **(cm²/Vs)**	25	210	25	25
N_A **(1/cm³)**	1.0E+16	0	0	0
N_D **(1/cm³)**	0	1.0E+18	1.0E+16	1.0E+18

Table 3. Parameter set for the optimized CIGS/In_2S_3/ZnO solar cell.

According to the simulation results, the absorber and window layer energy band gaps of the best experimental CIGS/In_2S_3/i-ZnO/ZnO/Al solar cells with 16.4% output efficiency should have been in the range of 1.14–1.27 eV and 3.42–3.68 eV, respectively. In the color map, the cell performance was defined as an order of triple made of absorber layer's band gap, window layer's band gap and the cell's efficiency. Thus, each efficiency value in color map has specific

corresponding value for absorber and window layer's band gap. Consequently, some particular points were specified in **Figure 10** with the efficiency value of 16.4%, equal to the efficiency reported for the cell in the reference. For example, if the measured value for the CIGS layer band gap in the best experimental cell is 1.2 eV, its window layer's energy band gap should be 3.42 eV and 16.4% efficiency. In other case, using absorber layer with 1.14 or 1.27 eV band gap for the cell would lead to having a window layer with energy band gap of 3.68 eV and hence obtains 16.4% efficiency from the cell. These outcomes can be considered as the proof of simulation result validity (**Table 3**).

7. Conclusion

CIGS thin film solar cells background, its technological trend and current challenges are presented in this chapter. The optimized CIGS/In_2S_3/i-ZnO/ZnO/Al solar cell material properties are proposed based on simulation results. As the proof of simulation results' validity, the best cells experimented and reported with their parameters are collected. These collections of cell information from literature are simulated and investigated. Some material properties from experimental cells are not reported directly in the literatures but have been calculated and proposed in a range through SCAPS simulation. The analyses, modeling and examination of the simulations results have shown that the optimization of material properties are promising and can improve the cell efficiency.

Author details

Nima Khoshsirat[1] and Nurul Amziah Md Yunus[2*]

*Address all correspondence to: amziah@upm.edu.my

1 Science and Engineering Faculty, Queensland University of Technology, Brisbane, QLD, Australia

2 Micro and Nano Electronic Systems Unit (MiNES) and Advanced Material Synthesis and Fabrication Laboratory (AMSF), Department of Electrical and Electronic Engineering, Faculty of Engineering, Universiti Putra Malaysia (UPM), Serdang, Malaysia

References

[1] J. Poortmans and V. Arkhipov, *Thin film solar cells: fabrication, characterization and applications*, vol. 5. John Wiley & Sons, West Sussex, England, 2006.

[2] J. W. Arnulf, "Progress in chalcopyrite compound semiconductor research for photovoltaic applications and transfer of results into actual solar cell production," *Solar Energy Materials and Solar Cells,* vol. 95, pp. 1509–1517, 2011.

[3] L. A. Kosyachenko, *Solar cells thin-film technologies*. Rijeka, Croatia: InTech, 2011.

[4] L. L. Kazmerski. *Best research solar cell efficiencies*, 2016. Available: http://www.nrel.gov/ncpv/images/efficiency_chart.jpg

[5] M. Powalla, W. Witte, P. Jackson, S. Paetel, E. Lotter, R. Wuerz, *et al.*, "CIGS cells and modules with high efficiency on glass and flexible substrates," *Photovoltaics, IEEE Journal of*, vol. 4, pp. 440–446, 2014.

[6] M. A. Green, K. Emery, Y. Hishikawa, W. Warta, and E. D. Dunlop, "Solar cell efficiency tables (version 48)", *Progress in Photovoltaics: Research and Applications*, vol. 24, pp. 905–913, 2016.

[7] N. H. Rafat and S. E. D. Habib, "The limiting efficiency of band gap graded solar cells," *Solar Energy Materials and Solar Cells*, vol. 55, pp. 341–361, 9/4/1998.

[8] S. Niki, M. Contreras, I. Repins, M. Powalla, K. Kushiya, S. Ishizuka, *et al.*, "CIGS absorbers and processes," *Progress in Photovoltaics: Research and Applications*, vol. 18, pp. 453–466, 2010.

[9] N. Khoshsirat, N. A. Md Yunus, M. N. Hamidon, S. Shafie, and N. Amin, "Analysis of absorber layer properties effect on CIGS solar cell performance using SCAPS," *Optik – International Journal for Light and Electron Optics*, vol. 126, pp. 681–686, 4/2015.

[10] L. Assmann, J. C. Bernède, A. Drici, C. Amory, E. Halgand, and M. Morsli, "Study of the Mo thin films and Mo/CIGS interface properties," *Applied Surface Science*, vol. 246, pp. 159–166, 2005.

[11] S.-Y. Kuo, L.-B. Chang, M.-J. Jeng, W.-T. Lin, Y.-T. Lu, and S.-C. Hu, "Effects of Growth Parameters on Surface-morphological, Structural and Electrical Properties of Mo Films by RF Magnetron Sputtering", *MRS Online Proceedings Library*, vol. 1123, pp. 1123–P05, 2008.

[12] W. Witte, R. Kniese, and M. Powalla, "Raman investigations of $Cu(In,Ga)Se_2$ thin films with various copper contents," *Thin Solid Films*, vol. 517, pp. 867–869, 11/28/2008.

[13] O. Lundberg, J. Lu, A. Rockett, M. Edoff, and L. Stolt, "Diffusion of indium and gallium in $Cu(In,Ga)Se_2$ thin film solar cells," *Journal of Physics and Chemistry of Solids*, vol. 64, pp. 1499–1504, 2003.

[14] B. McCandless and S. Hegedus, "Influence of CdS window layers on thin film CdS/CdTe solar cell performance," in *Photovoltaic Specialists Conference, Conference Record of the Twenty Second IEEE*, Las Vegas, NV, US, 1991, pp. 967–972.

[15] M. A. Contreras, M. J. Romero, B. To, F. Hasoon, R. Noufi, S. Ward, *et al.*, "Optimization of CBD CdS process in high-efficiency Cu(In,Ga)Se2-based solar cells," *Thin Solid Films*, vol. 403–404, pp. 204–211, 2002.

[16] U. Rau and H. W. Schock, "llc-4 – Cu(In,Ga)Se2 thin-film solar cells," in *Solar Cells*, M. Tom and C. Luis, Eds. Oxford: Elsevier Science, 2005, pp. 303–349.

[17] R.A. Mickelsen and WS Chen, "Development of a 9.4% efficient thin-film CuInSe2/CdS solar cell," presented at *the 15th IEEE Photovoltaic Specialists Conference*, New York, USA, 1981.

[18] S. Siebentritt, "Alternative buffers for chalcopyrite solar cells," *Solar Energy*, vol. 77, pp. 767–775, 2004.

[19] A. Romeo, M. Terheggen, D. Abou-Ras, D. L. Bätzner, F. J. Haug, M. Kälin, *et al.*, "Development of thin-film Cu(In,Ga)Se_2 and CdTe solar cells," *Progress in Photovoltaics: Research and Applications*, vol. 12, pp. 93–111, 2004.

[20] R. Klenk and M. C. Lux-Steiner, "Chalcopyrite based solar cells," in Thin Film Solar Cells: Fabrication, Characterization and Applications, *John Wiley & Sons, Ltd, West Sussex, UK*, pp. 237-275, 2006.

[21] D. Hariskos, S. Spiering, and M. Powalla, "Buffer layers in Cu(In,Ga)Se_2 solar cells and modules," *Thin Solid Films*, vol. 480–481, pp. 99–109, 2005.

[22] D. Ginley. and J. Perkins., "Transparent conducting oxides for advanced photovoltaic applications," *Photovoltaics International Journal*, 3rd edition, pp. 95–102, February 2009.

[23] M. Izaki and T. Omi, "Transparent zinc oxide films prepared by electrochemical reaction," *Applied Physics Letters*, vol. 68, pp. 2439–2440, 1996.

[24] T. Minami, H. Sato, H. Nanto, and S. Takata, "GROUP III Impurity Doped Zinc Oxide Thin Films Prepared By RF Magnetron Sputtering," *Japanese Journal of Applied Physics*, Part 2: Letters, vol. 24, pp. 781–784, 1985.

[25] J. J. Loferski, "Theoretical considerations governing the choice of the optimum semiconductor for photovoltaic solar energy conversion," *Journal of Applied Physics*, vol. 27, pp. 777–784, 1956.

[26] V. Avrutin, N. Izyumskaya, and H. Morkoç, "Semiconductor solar cells: recent progress in terrestrial applications," *Superlattices and Microstructures*, vol. 49, pp. 337–364, 2011.

[27] R. Scheer, "Activation energy of heterojunction diode currents in the limit of interface recombination," *Journal of Applied Physics*, vol. 105, p. 4505, 2009.

[28] A. Niemegeers, M. Burgelman, and A. De Vos, "On the CdS/$CuInSe_2$ conduction band discontinuity," *Applied Physics Letters*, vol. 67, pp. 843–845, 1995.

http://dx.doi.org/10.5772/64166

[29] L. A. Kosyachenko, "A Theoretical Description of Thin-Film Cu(In,Ga)Se2 Solar Cell Performance," in *Solar Cells - New Approaches and Reviews*, ed: Leonid A. Kosyachenko, INTECH, Croatia, 2015.

[30] Z.-H. Li, E.-S. Cho, and S. J. Kwon, "Molybdenum thin film deposited by in-line DC magnetron sputtering as a back contact for Cu(In,Ga)Se_2 solar cells," *Applied Surface Science*, vol. 257, pp. 9682–9688, 2011.

[31] M. Edoff, N. Viard, J. T. Wätjen, S. Schleussner, P.-O. Westin, and K. Leifer, "Sputtering of highly adhesive Mo back contact layers for Cu(In,Ga)Se2 solar cells," presented at the *24th European Photovoltaic Solar Energy Conference*, München, Germany, 2009.

[32] H.-W. Schock, "Properties of chalcopyrite-based materials and film deposition for thin-film solar cells," in *Thin-Film Solar Cells*, ed: Springer, Berlin, 2004, pp. 163–182.

[33] K. Seshan, Handbook of thin film deposition: *William Andrew, Elsevier*, UK, 2012.

[34] D. B. Mitzi, M. Yuan, W. Liu, A. J. Kellock, S. J. Chey, L. Gignac, *et al.*, "Hydrazine-based deposition route for device-quality CIGS films," *Thin Solid Films*, vol. 517, pp. 2158–2162, 2009.

[35] M. G. Faraj, K. Ibrahim, and A. Salhin, "Fabrication and characterization of thin-film Cu (In, Ga) Se2 solar cells on a PET plastic substrate using screen printing," *Materials Science in Semiconductor Processing*, vol. 15, pp. 165–173, 2012.

[36] D.-Y. Lee, S. Park, and J. Kim, "Structural analysis of CIGS film prepared by chemical spray deposition," *Current Applied Physics*, vol. 11, pp. S88–S92, 2011.

[37] M. Kaelin, D. Rudmann, F. Kurdesau, H. Zogg, T. Meyer, and A. N. Tiwari, "Low-cost CIGS solar cells by paste coating and selenization," *Thin Solid Films*, vol. 480, pp. 486–490, 2005.

[38] T. Nakada and S. Shirakata, "Impacts of pulsed-laser assisted deposition on CIGS thin films and solar cells," *Solar Energy Materials and Solar Cells*, vol. 95, pp. 1463–1470, 2011.

[39] V. S. Saji, I.-H. Choi, and C.-W. Lee, "Progress in electrodeposited absorber layer for $CuIn_{(1-x)}GaxSe_2$ (CIGS) solar cells," *Solar Energy*, vol. 85, pp. 2666–2678, 2011.

[40] Y. Hamakawa, Thin-film solar cells: next generation photovoltaics and its applications vol. 13: *Springer Science & Business Media*, Berlin 2004.

[41] Y. Hashimoto, "Chemical bath deposition of CdS buffer layer for CIGS solar cells," *Solar Energy Materials and Solar Cells*, vol. 50, pp. 71–77, 1998.

[42] A. Ennaoui, M. Weber, R. Scheer, and H. Lewerenz, "Chemical-bath ZnO buffer layer for CuInS 2 thin-film solar cells," *Solar Energy Materials and Solar Cells*, vol. 54, pp. 277–286, 1998.

[43] J. F. Trigo, B. Asenjo, J. Herrero, and M. T. Gutiérrez, "Optical characterization of In_2S_3 solar cell buffer layers grown by chemical bath and physical vapor deposition," *Solar Energy Materials and Solar Cells*, vol. 92, pp. 1145–1148, 2008.

[44] N. Naghavi, R. Henriquez, V. Laptev, and D. Lincot, "Growth studies and characterisation of In_2S_3 thin films deposited by atomic layer deposition (ALD)," *Applied Surface Science*, vol. 222, pp. 65–73, 2004.

[45] S. Siebentritt, P. Walk, U. Fiedeler, I. Lauermann, K. Rahne, M. C. Lux-Steiner, *et al.*, "MOCVD as a dry deposition method of ZnSe buffers for $Cu(In,Ga)(S,Se)_2$ solar cells," *Progress in Photovoltaics: Research and Applications*, vol. 12, pp. 333–338, 2004.

[46] L. Gao, Y. Zhang, J.-M. Zhang, and K.-W. Xu, "Boron doped ZnO thin films fabricated by RF-magnetron sputtering," *Applied Surface Science*, vol. 257, pp. 2498–2502, 2011.

[47] R. Menner, D. Hariskos, V. Linss, and M. Powalla, "Low-cost ZnO:Al transparent contact by reactive rotatable magnetron sputtering for $Cu(In,Ga)Se_2$ solar modules," *Thin Solid Films*, vol. 519, pp. 7541–7544, 2011.

[48] K.-m. Lin and P. Tsai, "Parametric study on preparation and characterization of ZnO:Al films by sol–gel method for solar cells," *Materials Science and Engineering: B*, vol. 139, pp. 81–87, 2007.

[49] D. Kim, I. Yun, and H. Kim, "Fabrication of rough Al doped ZnO films deposited by low pressure chemical vapor deposition for high efficiency thin film solar cells," *Current Applied Physics*, vol. 10, pp. S459–S462, 2010.

[50] L. Cao, L. Zhu, J. Jiang, R. Zhao, Z. Ye, and B. Zhao, "Highly transparent and conducting fluorine-doped ZnO thin films prepared by pulsed laser deposition," *Solar Energy Materials and Solar Cells*, vol. 95, pp. 894–898, 2011.

[51] J. Rousset, F. Donsanti, P. Genevée, G. Renou, and D. Lincot, "High efficiency cadmium free $Cu(In,Ga)Se_2$ thin film solar cells terminated by an electrodeposited front contact," *Solar Energy Materials and Solar Cells*, vol. 95, pp. 1544–1549, 2011.

[52] O. Kluth, G. Schöpe, B. Rech, R. Menner, M. Oertel, K. Orgassa, *et al.*, "Comparative material study on RF and DC magnetron sputtered ZnO: Al films," *Thin Solid Films*, vol. 502, pp. 311–316, 2006.

[53] M. Saad and A. Kassis, "Effect of rf power on the properties of rf magnetron sputtered ZnO: Al thin films," *Materials Chemistry and Physics*, vol. 136, pp. 205–209, 2012.

[54] R. Noufi, *CIGS PV technology – challenges, opportunities, and potential*. National Renewable Energy Laboratory. National Center for Photovoltaics, USA. 2013.

[55] Q. Cao, O. Gunawan, M. Copel, K. B. Reuter, S. J. Chey, V. R. Deline, *et al.*, "Defects in Cu (In, Ga) Se_2 chalcopyrite semiconductors: a comparative study of material properties, defect states, and photovoltaic performance," *Advanced Energy Materials*, vol. 1, pp. 845–853, 2011.

[56] J. Pohl, T. Unold, and K. Albe, "Antisite traps and metastable defects in Cu (In, Ga) Se_2 thin-film solar cells studied by screened-exchange hybrid density functional theory," *arXiv preprint arXiv:1205.2556*, 2012.

[57] B. Huang, S. Chen, H.-X. Deng, L.-W. Wang, M. A. Contreras, R. Noufi, *et al.*, "Origin of reduced efficiency in Cu (In, Ga) Se solar cells with high Ga concentration: alloy solubility versus intrinsic defects," *Photovoltaics, IEEE Journal of*, vol. 4, pp. 477–482, 2014.

[58] EC-2002a, "Directive 2002/95/EC of the European Parliament and of the Council of 27 January 2003 on the restriction of the use of certain hazardous substances in electrical and electronic equipment," *Official Journal of the European Union*, vol. L 37, pp. 19–23, 2003.

[59] EC-2002b, "Directive 2002/96/EC of the European Parliament and of the Council of 27 January 2003 on waste electrical and electronic equipment," *Official Journal of the European Union*, vol. L 37, pp. 24–38, 2003.

[60] R. Ortega Borges, D. Lincot, and J. Vedel, "Chemical bath deposition of zinc sulfide thin films," *Proceedings of the 11th EC PVSEC, Montreux, Switzerland*, pp. 862–865, 1992.

[61] C. Huang, S. S. Li, W. Shafarman, C.-H. Chang, E. Lambers, L. Rieth, *et al.*, "Study of Cd-free buffer layers using In x (OH, S) y on CIGS solar cells," *Solar Energy Materials and Solar Cells*, vol. 69, pp. 131–137, 2001.

[62] N. Barreau, S. Marsillac, D. Albertini, and J. Bernede, "Structural, optical and electrical properties of β-In2S3-3xO3x thin films obtained by PVD," *Thin Solid Films*, vol. 403, pp. 331–334, 2002.

[63] E. Yousfi, T. Asikainen, V. Pietu, P. Cowache, M. Powalla, and D. Lincot, "Cadmium-free buffer layers deposited by atomic later epitaxy for copper indium diselenide solar cells," *Thin Solid Films*, vol. 361, pp. 183–186, 2000.

[64] N. A. Allsop, A. Schönmann, H. J. Muffler, M. Bär, M. C. Lux-Steiner, and C. H. Fischer, "Spray-ILGAR indium sulfide buffers for $Cu(In,Ga)(S,Se)_2$ solar cells," *Progress in Photovoltaics: Research and Applications*, vol. 13, pp. 607–616, 2005.

[65] S. Gall, N. Barreau, F. Jacob, S. Harel, and J. Kessler, "Influence of sodium compounds at the Cu (In, Ga) Se 2/(PVD) In_2S_3 interface on solar cell properties," *Thin Solid Films*, vol. 515, pp. 6076–6079, 2007.

[66] D. Hariskos, R. Menner, S. Spiering, A. Eicke, M. Powalla, K. Ellmar, *et al.*, "In_2S_3 buffer layer deposited by magnetron sputtering for Cu (InGa) Se2 solar cells," in *Proc. Solar Energy Conference*, New Orleans, US, 2004.

[67] M. R. Hariskos D, Lotter E, Spiering S, Powalla M., "Magnetron sputtering of indium sulphide as the buffer layer in $Cu(InGa)Se_2$-based solar cells.," in *20th European Photovoltaic Solar Energy Conference, Barcelona, Spain*, 2005.

[68] N. Khoshsirat and N. A. M. Yunus, "Numerical Simulation of CIGS Thin Film Solar Using SCAPS-1D," presented at *the 2013 IEEE Conference on Sustainable Utilization and Development in Engineering and Technology*, Putrajaya, Malaysia, 2013.

[69] M. I. Hossain, "Fabrication and characterization of CIGS solar cells with In_2S_3 buffer layer deposited by PVD technique," *Chalcogenide Letters*, vol. 9, pp. 185–191, 2012.

[70] J. Sterner, J. Malmstr[??]m, and L. Stolt, "Study on ALD In_2S_3/Cu(In,Ga)Se_2 interface formation," *Progress in Photovoltaics: Research and Applications*, vol. 13, pp. 179–193, 2005.

[71] S. Spiering, L. Bürkert, D. Hariskos, M. Powalla, B. Dimmler, C. Giesen, *et al.*, "MOCVD indium sulphide for application as a buffer layer in CIGS solar cells," *Thin Solid Films*, vol. 517, pp. 2328–2331, 2009.

[72] H. A. Maksoud, M. Igalson, and S. Spiering, "Influence of post-deposition heat treatment on electrical transport properties of In_2S_3-buffered Cu (In, Ga) Se 2 cells," *Thin Solid Films*, vol. 535, pp. 158–161, 2013.

[73] S. Gall, N. Barreau, S. Harel, J. Bernede, and J. Kessler, "Material analysis of PVD-grown indium sulphide buffer layers for Cu(In, Ga)Se_2-based solar cells," *Thin Solid Films*, vol. 480, pp. 138–141, 2005.

[74] S. Spiering, D. Hariskos, M. Powalla, N. Naghavi, and D. Lincot, "CD-free Cu(In,Ga)Se_2 thin-film solar modules with In_2S_3 buffer layer by ALCVD," *Thin Solid Films*, vol. 431–432, pp. 359–363, 2003.

[75] S. Spiering, A. Eicke, D. Hariskos, M. Powalla, N. Naghavi, and D. Lincot, "Large-area Cd-free CIGS solar modules with In_2S_3 buffer layer deposited by ALCVD," *Thin Solid Films*, vol. 451, pp. 562–566, 2004.

[76] W. Vallejo, J. Clavijo, and G. Gordillo, "CGS based solar cells with In_2S_3 buffer layer deposited by CBD and coevaporation," *Brazilian Journal of Physics*, vol. 40, pp. 30–37, 2010.

[77] N. Khoshsirat, N. A. Md Yunus, M. N. Hamidon, S. Shafie, and N. Amin, "Analysis of absorber and buffer layer band gap grading on CIGS thin film solar cell performance using SCAPS," *Pertanika Journal of Science an Technology*, vol. 23, pp. 241–250, 2015.

[78] N. Khoshsirat and N. A. M. Yunus, "Numerical Simulation of CIGS Thin Film Solar Using SCAPS-1D," presented at *the 2013 IEEE Conference on Sustainable Utilization and Development in Engineering and Technology*, Putrajaya, Malaysia, 2013.

[79] N. Khoshsirat, N. A. Md Yunus, H. M. Nizar, S. Shafie, and N. Amin, "Optimization of CIGS Thin Film Solar Cells via Numerical Simulation," in *INTERNATIONAL SYMPOSIUM ON APPLIED ENGINEERING AND SCIENCES (SAES 2013)*, UPM, Serdang Malaysia, 2013.

[80] N. Khoshsirat, N. Md Yunus, M. N. Hamidon, S. Shafie, and N. Amin, "ZnO doping profile effect on CIGS solar cells efficiency and parasitic resistive losses based on cells

equivalent circuit," in *2013 IEEE International Conference on Circuits and Systems (ICCAS)*, Kuala Lumpur, Malaysia, 2013, pp. 86–91.

[81] J. Pettersson, T. Torndahl, C. Platzer-Bjorkman, A. Hultqvist, and M. Edoff, "The influence of absorber thickness on Cu (In, Ga) Se solar cells with different buffer layers," *IEEE Journal of Photovoltaics*, vol. 3, pp. 1376–1382, 2013.